



Investigation of the Effect of Sintering Temperatures on the Production of Porous NiTi Alloy by Loosen Sintering Method

Naci Arda Tanış¹ , Bülent Bostan² 

¹ Department of Metallurgy and Materials Engineering, Kırıkkale University, 71450 Kırıkkale, TURKEY

² Department of Metallurgy and Materials Engineering, Gazi University, 06500 Ankara, TURKEY

Başvuru/Received: 19/10/2022

Kabul / Accepted: 25/11/2022

Çevrimiçi Basım / Published Online: 20/12/2022

Son Versiyon/Final Version: 31/01/2022

Abstract

This article aims to produce NiTi shape memory alloys, which show superelasticity and shape memory effect, as well as good biocompatibility and corrosion properties, in open and porous sizes ranging from 100-500 μm , which are required for use as implants. This structure of pores is necessary to allow tissue growth and fluid flow inside the implants. Many powder metallurgy methods have been used in producing porous NiTi shape memory alloys. However, the packaging pressure used in these methods has not successfully created the desired pore distribution, shape, and size. The methods by which it can be produced are costly in terms of cost. In the study, production was carried out by sintering the powder mixture poured into molds without pressure with the help of binder polymers. This sintering process was carried out in an argon atmosphere for 1 hour at temperatures 1050, 1125, and 1200 °C. The study shows that pressureless loosen sintering can produce porous NiTi alloys, which is the more straightforward method. The pore distribution and proportions were examined. Homogeneous distribution and pores in desired sizes are created. It has also been determined that the binder polymer has a space-retaining effect. It was determined at which temperature the alloy sintered at different temperatures contained the desired B2 austenite phase for superelasticity. Austenite start and finish temperatures were determined for the alloy produced at each sintering temperature. As a result of this research, it was determined which phase was denser at which temperature, and the phase transformation temperatures were found. This method will decrease production costs, and more people will have access to this material. In general, the mechanism of sintering methods is joining the points in contact with the packaging pressure by necking. In this study, the combination of the grains with the polymer without packaging pressure with the thermal expansion mechanism reveals the originality of the study.

Key Words

“NiTi, Shape Memory Alloy, Powder Metallurgy, Porosity”

1. Introduction

NiTi alloys have superelastic and shape memory properties with combinations of thermoelastic transformation, acicular Ni₄Ti₃ phase, and twinning mechanisms. Thanks to its unique properties, good mechanical strength, relatively low elastic modulus, low corrosion resistance, and biocompatibility, it has a wide usage area in many sectors such as automotive, aerospace, aviation, medical, and implant (Lu et al., 2021). The elastic modulus of the bulk NiTi alloys used as implants in the human body is higher than the elastic modulus of the bones, making load transfer between the implant and the bone difficult. This situation causes local osteoporosis, which causes tissue loss in the bone called “stress shield” (LAI et al., 2021; Yuan et al., 2018). In order to eliminate such negativities, studies on NiTi alloys to reduce their density and elastic modulus by controlling their pores have been increasing recently. For example, reducing the mass weight in aircraft (Li et al., 2010) and reducing the stress shielding effect in implant applications (Bansiddhi et al., 2008) make this material very useful. In addition to reducing the stress shielding effect, porous implants should be able to grow in bone tissues and provide fluid passage within the implant (Xu et al., 2014). NiTi open-pore materials fulfill the requirements for implants. The first of these needs is that NiTi alloys show close biocompatibility compared to stainless steel and titanium. Second, it should provide a good combination of high strength to prevent deformation and cracks, relatively low hardness from reducing stress shielding, and high toughness to avoid brittle fractures. Finally, it provides good mechanical stability with bone tissue (Bansiddhi et al., 2008).

NiTi phase has a lower enthalpy of formation compared to other intermetallic phases. Elemental or pre-alloyed powders are used in the production of porous NiTi. However, using elemental powders, sintering methods cause incomplete NiTi formation because it takes place at low temperatures. This causes the formation of intermetallic phases such as Ni₃Ti and Ti₂Ni. These phases are difficult to remove even after prolonged high-temperature homogenization processes. Researchers have recently started using pre-alloyed NiTi powders to prevent this (Bansiddhi et al., 2008)

Since NiTi has a high melting point (1310 °C), the production of porous materials has been carried out by powder metallurgy methods. For the porous NiTi produced, the powder can be in elemental or pre-alloyed form. Many methods have been investigated to produce porous NiTi alloys with P/M. These methods are spark plasma sintering (SPS) (Özerim et al., 2022), self-propelled temperature synthesis (SHS) (Wisutmethangoon et al., 2009), hot isostatic pressing (HIP) (Farvizi et al., 2018), microwave sintering (MWS) (Xu et al., 2014), and additive manufacturing (AM) (M. Zhao et al., 2021). However, these production methods are generally expensive, and difficult to control the pore structure and shape. In addition, these methods are not very suitable for the production of complex shaped structures and mass production.

Researchers have recently used pore-forming methods by mixing space-retaining materials and powders to produce porous NiTi and then evaporate these powders. For example, NaCl (X. Zhao et al., 2009) in metal injection molding, NaF (Bansiddhi & Dunand, 2007) in hot-isostatic pressing, NH₄HCO₃ (Zhang et al., 2015) in free capsule hot isostatic pressing, and Mg in microwave sintering (LAI et al., 2021). In these studies, pressures between 100 and 700 MPa are applied for the packaging of powders. Due to the applied pressure, producing open pores of 100 – 500 microns is challenging, which is required for a porous implant. The intergranular channels connecting the large pores are closed by the packing pressure.

In powder metallurgy methods, sintering takes place by two different mechanisms, the necking of the grains in contact with the pressure at the contact points or the expansion of the grains during the sintering process and their union from these points by necking. In this study, the mechanism of grain expansion was used instead of the mechanism of grains in contact with the pressure used in traditional methods. By giving the NiTi powders fluidity with a binder, it is ensured that the molds take shape, then with the help of the same binder, pore formation and the raw sample remain in a bulk form. After sintering, the metallographic characterization of the samples was carried out.

2. Materials and Methods

In this study, eq.-atomic pre-alloyed NiTi powders obtained from the company (Nanoval GmbH) with an average grain size of 34 µm were used to produce porous NiTi samples. Firstly, NiTi powders were mixed with a binder mixture containing 83% PEG, 15% PP, and 2% SA in a turbo mixer at a ratio of 1:2 for one hour. The prepared mixture was then mixed for 30 minutes at 90 °C and poured into cylindrical molds with a diameter of 12 mm. The cooled samples in the molds were then removed in a cylindrical shape. In order to recover PEG from the extracted raw samples, the samples were kept in water at room temperature for one day, and the PEG polymer was removed from the sample. After the debinding process, dried samples were sintered for 1 hour at each temperature at 1050, 1125, and 1200 °C, respectively. During sintering, Ar gas was given to the furnace atmosphere from one end, and the tube was taken from the other end of the chamber. During this process, PP and SA were gasified between 300-500 C and removed from the system. The cylindrical geometry of the sintered samples was used to measure the porosity ratios. For this purpose, their actual densities were determined by using the volume/density formula (Eq. 1.1), and pore ratios were determined with Equation 1.2;

$$\rho_{true} = \frac{m}{V} \quad (1)$$

$$\%Porosity = \frac{\rho_{theoretical} - \rho_{true}}{\rho_{theoretical}} \times 100 \quad (2)$$

In Equation 1.1, m is the mass of the sample, and V is the volume of the sample. P is the theoretical density of the material considered to be fully charged, and ρ is the theoretical, actual post-production density of the material.

After calculating their densities and pore ratios, the samples were examined under an optical microscope to see the microstructure and pore distribution. Samples, sanding, and polishing operations were performed for microstructure examination. It was then etched in HF, HNO₃, and sterile water solution. The distribution and chemical analysis of the phases in the material microstructure were calculated using scanning electron microscopy (SEM) and electron diffraction spectrometry (EDS) devices. After these microstructure analyses, analyses on X-ray diffraction (XRD) were carried out to calculate the composition of the phases formed at different sintering temperatures from 20 to 90° 2 θ . To determine how the austenite start and end temperatures are affected by sintering temperatures, analyzes were performed on a differential scanning calorimetry (DSC) device.

3.Results and Discussions

Figure 1 gives optical microscope images of NiTi powders mixed with a binder (PEG 8000, PP, and SA) after molding, before, and after debinding. When we look at the material surface before debinding, it is seen that the PEG 8000 polymer spreads in certain areas in the microstructure at an average size of 100 - 300 microns, and this spread was homogeneous. In Figure 1. b, when the images of the same sample after sintering at 1125 C for 1 hour are analyzed, it is seen that pores are formed in the regions where PEG 8000 polymer is present. These pores are connected by the channels formed by the volatilization of PP and SA around the NiTi powder grains in the thermal polymer removal process before sintering. It is seen that they form necking zones from the contact at 1125 °C 1 hour and merge from these points.

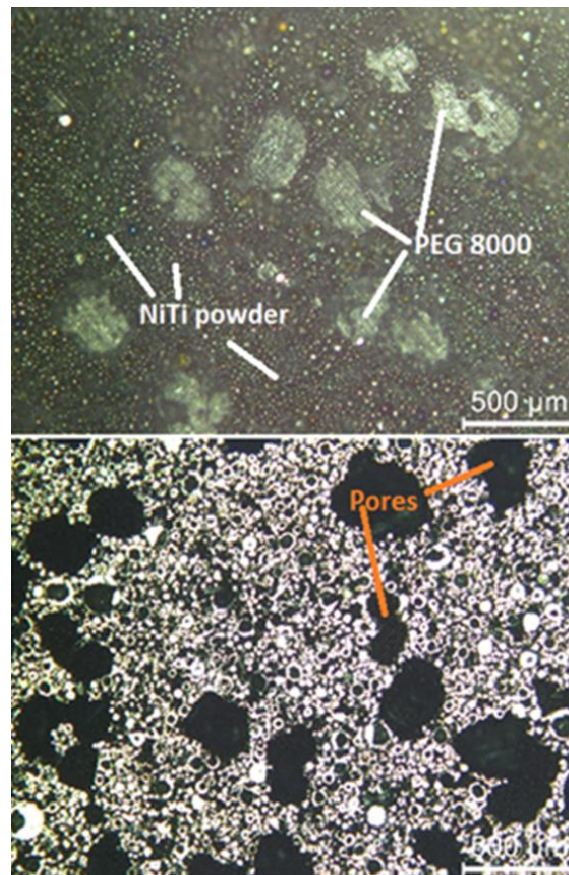


Figure 1. (a) Optical microscope image of the raw sample before the debinding process, (b) Optical microscope image of the sample sintered in Ar atmosphere at 1125 C for 1 hour

Considering the porosity rates given in Table 1 of the samples sintered in Ar atmosphere for 1 hour at 1050, 1125, and 1200 °C, it is seen that the porosity varies between 44-47% in all samples. It was determined that the main factor in pore formation was the binder/NiTi ratio in the initial feed mixture, and the temperature did not affect the overall porosity much.

Table.1. Densities and pore ratios of the samples produced by the non-pressure powder metallurgy method

Sample	Height (mm)	Diameter (mm)	Weight (g)	Volume (cm ³)	True Density (g/cm ³)	Theoretical Density (g/cm ³)	Porosity (%)
1050-1	13,63	12	5,5583	1,540	3,607	6,45	44,06
1125-1	15,14	12	5,9528	1,711	3,478	6,45	46,07
1200-1	9,04	12	3,6084	1,022	3,531	6,45	45,25

In Figure 2, SEM micrographs of the samples sintered for 1 hour at 1050, 1125, and 1200 °C are given at x1000 magnification. When these images were analyzed, it was determined that the dark gray part was the Ti-rich phase, the light gray part was the Ni-rich phase, and the gray part was the NiTi phase, as shown in the EDS analysis given in Figure 4. The NiTi phase is generally dominant in the structure in the pre-alloyed NiTi powders used before the process. However, increasing temperature, it has been determined that with the diffusion of Ni and Ti atoms in the NiTi alloys, especially Ni₃Ti, a NiTi₂ phase with Ti moving away from the structure is formed in the previous studies. It has been determined that as you go from the grain center to the grain boundary, firstly, the Ni₃Ti phase is formed, the increasing Ti atoms from there move to the grain boundary or the pore edges to form the Ti₂Ni phase. When this phase becomes stable, the increasing Ti atoms accumulate at the grain boundaries and form a Ti-rich phase. This diffusion event increases with time within 1 hour. When the SEM micrograph of the sample sintered at 1050 °C in Figure 3a is examined, it is seen that the gray NiTi phase covers a large area. In the sample sintered at 1125 °C in Figure 3b, the ratio of this NiTi phase decreases, and the ratio of Ni₃Ti and Ti-rich phase increases. It was observed that the NiTi phase almost completely disappeared in the sample sintered at 1200 °C. When we look at the bonding rate of the grains, it is seen that the Ti atoms in the Ti-rich phases at the grain boundary of the coalescence are displaced by the other atoms in the grain boundary, and diffusion occurs thanks to this realized diffusion process. When the dimensions of the neck region are examined, it is seen that the necking grooves are not fully completed at 1050 °C, but the grains come into contact with each other. When the SEM micrograph of the sample sintered at 1125 °C is examined, it is seen that these grains are in better contact with each other, the neck regions are wider, and there is better coalescence. In the sample sintered at 1200 °C, it was determined that the sintering took place completely, and the neck regions disappeared. Only the Ti-rich dark gray region remained at the grain boundaries. It is undesirable in producing open-pore NiTi because the pores connected by the channels around the complete union become closed. In the same way, in the sintering of press-prepared green samples at 1050 °C, Ismail et al., (2012) In their study, the channels connecting each other around the pores were closed.

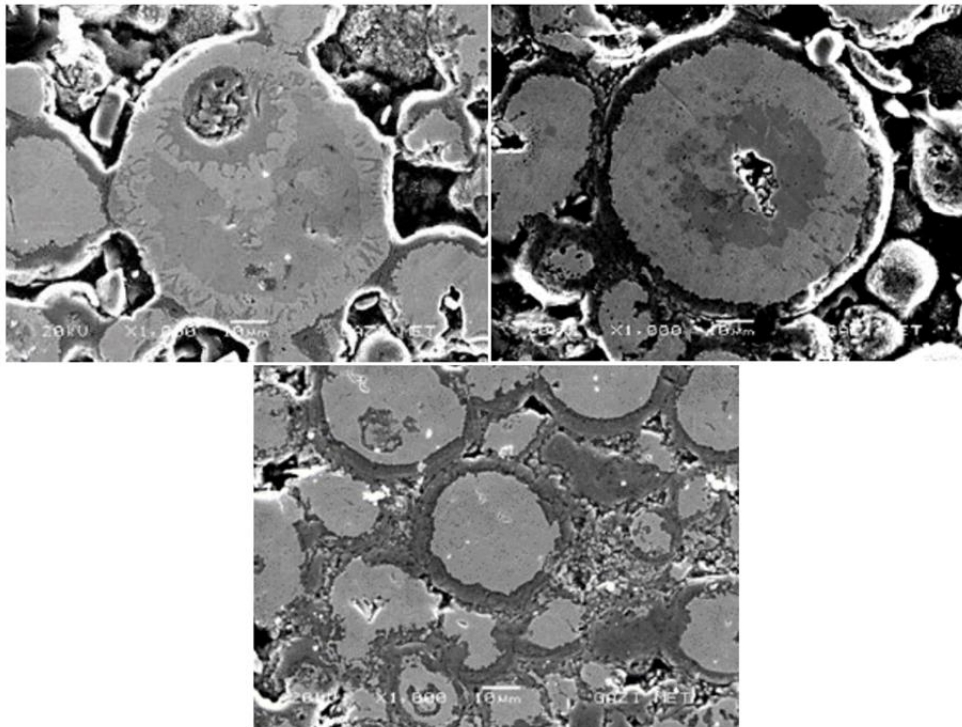


Figure 2. SEM micrograph of NiTi samples sintered for 1 hour a) 1050 C, b) 1125 C c) 1200 C

When looking at the micrograph analyses given in Figure 2, it was observed that closed pores were formed in the grain. The reason for these pores is explained as the formation of cavities in the center with an expansion of the grain after diffusion from the grain center to the grain boundaries. These spaces are called Kirkendall spaces. Yost et al., (2019) In their study on Ti coating on nickel wires, determined that the Kirkendall effect formed pores due to the diffusion mechanism between Ni-Ti. In this study, pores were formed due to diffusion between Ni-Ti.

The point EDS analysis of the sample sintered at 1125 C for 1 hour is given in Figure 3. In the point analysis taken from the center of the grain, Ni and Ti atoms are networked. 46.7% Ti and wt. 53.3% Ni was detected. It is possible to talk about the nearly equiatomic NiTi phase in this region. The Ti ratio is net in the point analysis taken from the light gray part away from the grain center, 36.5%, Ni content wt. 63.5% was found. When compared atomically according to the phase diagram, it was determined that the Nickel-rich phase was formed, but at this point, there was not precisely the Ni₃Ti stable phase. Any oxygen was found in the point analyses taken from these regions. In the elemental analysis, the mesh is at the necking point of the grain, and the dark gray part is at the grain edge. 88% Ti, wt. 4.5% Ni and wt. 7.5% O elements were detected. Here, the Ti atom is pushed to the grain boundaries as a result of diffusion, first forming the NiTi₂ stable phase with Ni. However, some Ti ions remained free in the saturated solution. When the free Ti ions were removed from the sample Ar atmosphere, they reacted with O atoms to form titanium oxide. Paz y Puente & Dunand, (2018) in their study on NiTi wires, reached the exact elemental percentages at the same contrast values as a result of EDS and SEM analyses and defined the regions.

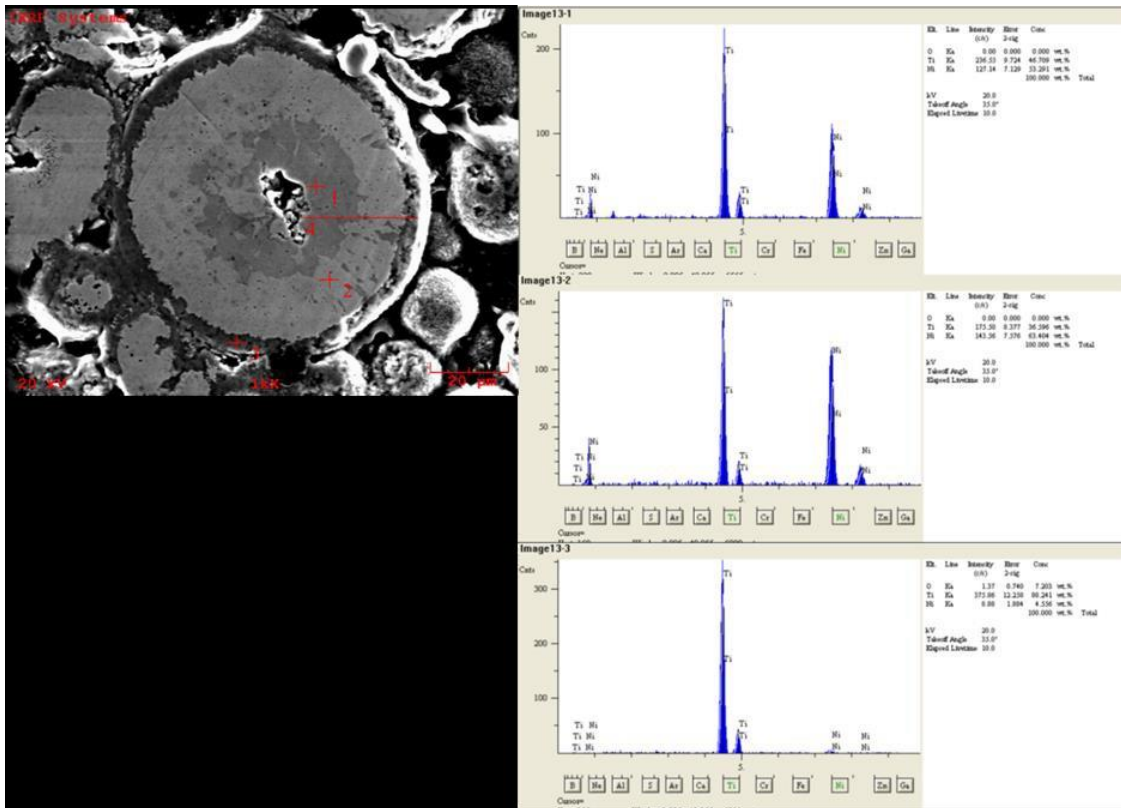


Figure 3. Point EDS analysis of the sample sintered in 1125 C 1 hour Ar atmosphere

XRD analyzes of the produced porous NiTi alloys are given in Figure 4. When the XRD peaks were examined, the peaks of the B19' martensite phase were observed at 1050 °C. The intensity of the B19' peaks decreased and disappeared at 1125 °C. The reason for that is thought to be the separation of Ti and Ni elements by diffusion and their transformation into stable Ti₂Ni and Ni₃Ti phases with the increasing temperature value. In the sample sintered at 1200 °C, the peaks of the B19' martensite phase were found again, which can be explained by the diffusion of Ti atoms in the Ti-rich phase at the grain boundary to the opposite grain and the transition to the Ni-rich phase with a lack of Ti concentration in the powders that diffusely merge at the grain boundaries. The peaks of the B2 austenite phase were observed at every temperature, especially at 1125 °C temperature, where the B19' phase was of low intensity, and the peak intensity increased. While the highest Ti₂Ni stable phase peak intensity was formed in the sample sintered at 1050 C, the peak intensity of this compound decreased with increasing temperature. While the peak intensity of the Ni₃Ti phase was found at the same degrees at 1050 and 1200 °C, it was determined that the intensity increased at 1125 °C compared to other temperatures. The increase in intensity at this temperature is due to the fact that there is more diffusion at 1050 °C, and there is no diffusion between the grains as at 1200 °C.

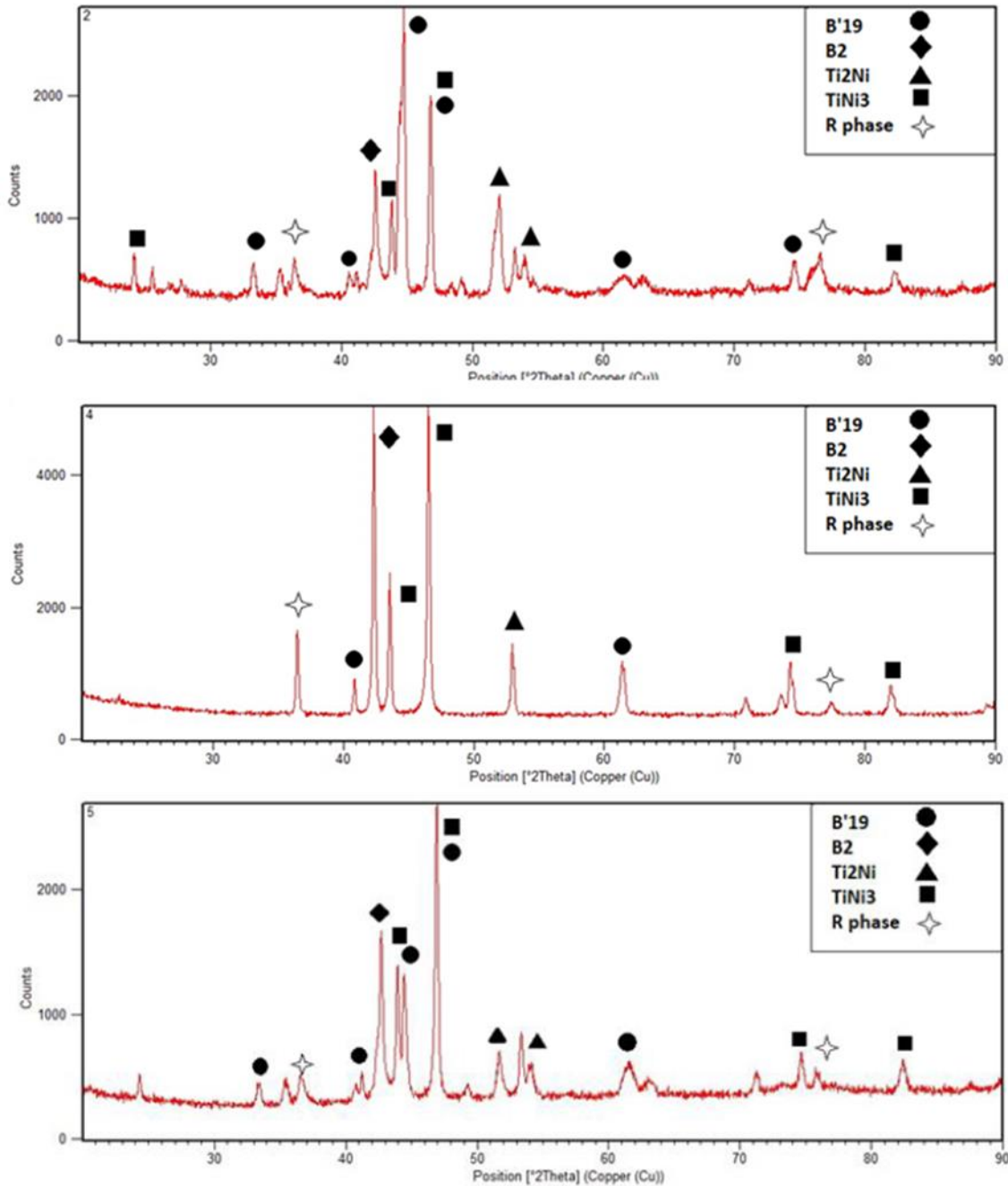


Figure 4. XRD analysis of samples produced by the non-pressure powder metallurgy method and sintered in Ar atmosphere for 1 hour (a) 1050 C, (b) 1125 C and (c) 1200 C

DSC analyzes of the samples were performed during heating. Analysis results are given in Figure 5. Considering the DSC analysis, the austenite initial temperature (A_s) of the porous NiTi alloy produced at 1050 °C was determined as 18.37 °C. The austenite finish temperature (A_f) was calculated as 91.1 °C. The austenite starting temperature of the sample produced at 1125 °C was found to be 13.4 °C, and the austenite ending temperature was 92.2 °C. Finally, the austenite starting temperature of the porous NiTi sample sintered at 1200 °C was found to be 16.6 °C, and the austenite ending temperature was determined as 90.3 °C. When the austenite start and end temperatures of the samples were examined, it was seen that these temperature values did not change much with the sintering temperature. In addition, the samples are not completely in the austenite phase at room temperature and contain a large amount of B19' martensite phase, as they are close to the austenite initial temperatures. Among the samples, the porous NiTi alloy sintered at 1125 °C for 1 hour showed the most accurate transformation behavior. The fact that the transformation range of the materials is extensive suggests that these materials are more prone to show superelasticity than shape memory properties. The XRD results given in Figure 4, on the other hand, support that the B2 phase will provide the most uniform transformation conditions due to the higher intensity of the sample sintered at 1125 °C and the low peaks of the other intermetallic phases.

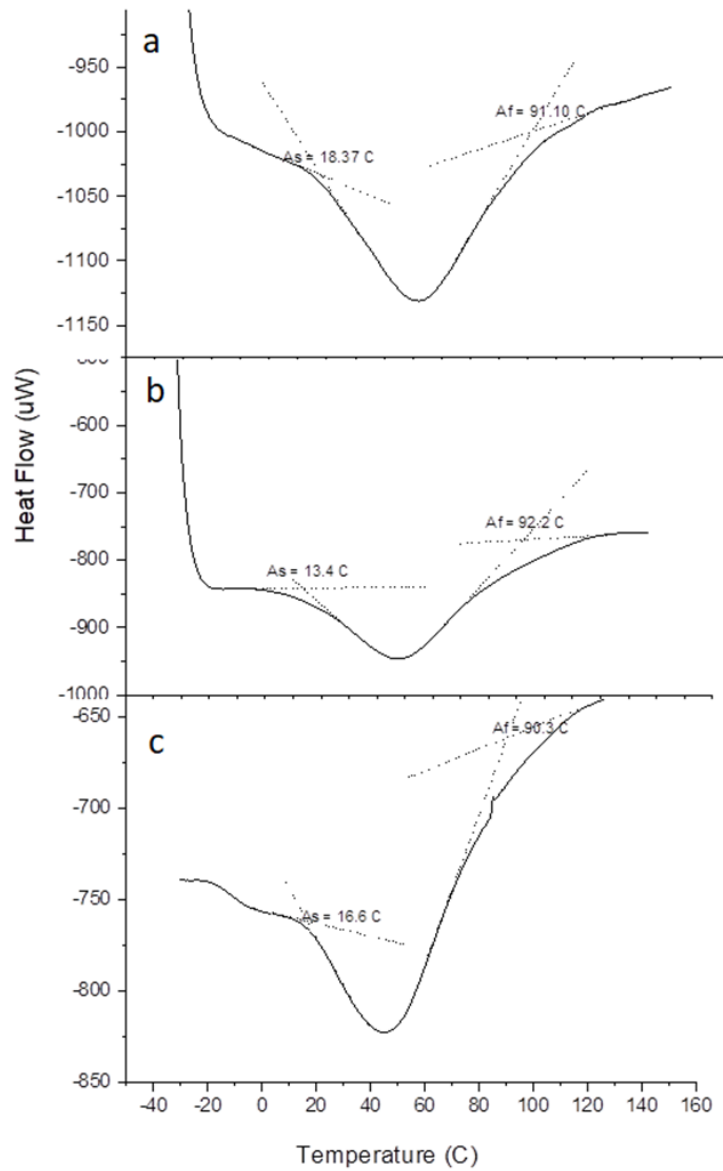


Figure 5. DSC curves of samples during heating (a) 1050 C, (b) 1125 C and (c) 1200 C

4. Conclusions

The study determined that the PEG 8000 polymer, which provides both space retention and fluidity, does its job and creates an open porous structure ranging from 100 to 500 microns. The pore measurements determined that there was not much change in the pore ratios with the sintering temperature, while the highest porosity was measured in the sample sintered at 1125 C for 1 hour. In SEM and EDS analyzes, it was determined that the diffusion process required for sintering was successful. In XRD analysis, while the peaks of B19' martensite phases were detected at 1050 °C and 1200 °C sintering temperatures, the B2 austenite phase was determined predominantly at 1125 °C. When we look at the DSC curves, it is seen that the sintering temperatures did not affect the austenite start and end temperatures of the sample. Still, the lowest austenite starting temperature and the highest austenite finish temperature were found for 1 hour of sintering at 1125 °C. In light of this study, it has been seen that the unpressurized system can produce porous NiTi shape memory alloys. In future studies, the samples to be made by this method were heat treated, paving the way for determining the phase structure and mechanical properties.

References

- Bansiddhi, A., & Dunand, D. C. (2007). Shape-memory NiTi foams produced by solid-state replication with NaF. *Intermetallics*, 15(12), 1612–1622. <https://doi.org/10.1016/J.INTERMET.2007.06.013>
- Bansiddhi, A., Sargeant, T. D., Stupp, S. I., & Dunand, D. C. (2008). Porous NiTi for bone implants: A review. *Acta Biomaterialia*, 4(4), 773–782. <https://doi.org/10.1016/J.ACTBIO.2008.02.009>
- Farvizi, M., Javan, M. K., Akbarpour, M. R., & Kim, H. S. (2018). Fabrication of NiTi and NiTi-nano Al₂O₃ composites by powder metallurgy methods: Comparison of hot isostatic pressing and spark plasma sintering techniques. *Ceramics International*, 44(13), 15981–15988. <https://doi.org/https://doi.org/10.1016/j.ceramint.2018.06.025>
- Ismail, M. H., Goodall, R., Davies, H. A., & Todd, I. (2012). Porous NiTi alloy by metal injection moulding/sintering of elemental powders: Effect of sintering temperature. *Materials Letters*, 70, 142–145. <https://doi.org/https://doi.org/10.1016/j.matlet.2011.12.008>
- LAI, T., XU, J., XIAO, Q., TONG, Y., HUANG, J., ZHANG, J., LUO, J., & LIU, Y. (2021). Preparation and characterization of porous NiTi alloys synthesized by microwave sintering using Mg space holder. *Transactions of Nonferrous Metals Society of China*, 31(2), 485–498. [https://doi.org/https://doi.org/10.1016/S1003-6326\(21\)65511-5](https://doi.org/https://doi.org/10.1016/S1003-6326(21)65511-5)
- Li, D. S., Zhang, X. P., Xiong, Z. P., & Mai, Y.-W. (2010). Lightweight NiTi shape memory alloy based composites with high damping capacity and high strength. *Journal of Alloys and Compounds*, 490(1–2). <https://doi.org/10.1016/j.jallcom.2009.10.025>
- Lu, H. Z., Ma, H. W., Luo, X., Wang, Y., Wang, J., Lupoi, R., Yin, S., & Yang, C. (2021). Microstructure, shape memory properties, and in vitro biocompatibility of porous NiTi scaffolds fabricated via selective laser melting. *Journal of Materials Research and Technology*, 15, 6797–6812. <https://doi.org/https://doi.org/10.1016/j.jmrt.2021.11.112>
- Özerim, G., Anlaş, G., & Moumni, Z. (2022). The effect of heat treatment on pseudoelastic behavior of spark plasma sintered NiTi. *Materials Today Communications*, 31, 103819. <https://doi.org/https://doi.org/10.1016/j.mtcomm.2022.103819>
- Paz y Puente, A. E., & Dunand, D. C. (2018). Synthesis of NiTi microtubes via the Kirkendall effect during interdiffusion of Ti-coated Ni wires. *Intermetallics*, 92, 42–48. <https://doi.org/https://doi.org/10.1016/j.intermet.2017.09.010>
- Wisutmethangoon, S., Denmud, N., & Sikong, L. (2009). Characteristics and compressive properties of porous NiTi alloy synthesized by SHS technique. *Materials Science and Engineering: A*, 515(1), 93–97. <https://doi.org/https://doi.org/10.1016/j.msea.2009.02.055>
- Xu, J. L., Jin, X. F., Luo, J. M., & Zhong, Z. C. (2014). Fabrication and properties of porous NiTi alloys by microwave sintering for biomedical applications. *Materials Letters*, 124, 110–112. <https://doi.org/https://doi.org/10.1016/j.matlet.2014.03.088>
- Yost, A. R., Erdeniz, D., y Puente, A. E. P., & Dunand, D. C. (2019). Effect of diffusion distance on evolution of Kirkendall pores in titanium-coated nickel wires. *Intermetallics*.
- Yuan, B., Zhu, M., & Chung, J. (2018). Biomedical Porous Shape Memory Alloys for Hard-Tissue Replacement Materials. *Materials*, 11, 1716. <https://doi.org/10.3390/ma11091716>
- Zhang, L., Zhang, Y. Q., Jiang, Y. H., & Zhou, R. (2015). Superelastic behaviors of biomedical porous NiTi alloy with high porosity and large pore size prepared by spark plasma sintering. *Journal of Alloys and Compounds*, 644, 513–522. <https://doi.org/10.1016/J.JALLCOM.2015.05.063>
- Zhao, M., Qing, H., Wang, Y., Liang, J., Zhao, M., Geng, Y., Liang, J., & Lu, B. (2021). Superelastic behaviors of additively manufactured porous NiTi shape memory alloys designed with Menger sponge-like fractal structures. *Materials & Design*, 200, 109448. <https://doi.org/https://doi.org/10.1016/j.matdes.2021.109448>
- Zhao, X., Sun, H., Lan, L., Huang, J., Zhang, H., & Wang, Y. (2009). Pore structures of high-porosity NiTi alloys made from elemental powders with NaCl temporary space-holders. *Materials Letters*, 63(28), 2402–2404. <https://doi.org/10.1016/J.MATLET.2009.07.069>